Applied Physics Letters

High figure-of-merit ultrathin metal transparent electrodes incorporating a conductive grid

Cite as: Appl. Phys. Lett. **96**, 041109 (2010); https://doi.org/10.1063/1.3299259
Submitted: 05 October 2009 . Accepted: 05 January 2010 . Published Online: 29 January 2010

D. S. Ghosh, T. L. Chen, and V. Pruneri

High figure-of-merit ultrathin metal transparent electrodes incorporating a conductive grid

D. S. Ghosh,[1,a)] T. L. Chen,[1,b)] and V. Pruneri[1,2]
[1]*ICFO-Institut de Ciències Fotòniques, Mediterranean Technology Park, Castelldefels, Barcelona, 08860 Catalunya, Spain*
[2]*ICREA-Institució Catalana de Recerca i Estudis Avançats, 08010 Barcelona, Spain*

(Received 5 October 2009; accepted 5 January 2010; published online 29 January 2010)

It is known that ultrathin (<10 nm) metal films (UTMFs) can achieve high level of optical transparency at the expense of the electrical sheet resistance. In this letter, we propose a design, the incorporation of an *ad hoc* conductive grid, which can significantly reduce the sheet resistance of UTMF based transparent electrodes, leaving practically unchanged their transparency. The calculated highest figure-of-merit corresponds to a filling factor and a grid spacing-to-linewidth ratio of 0.025 and 39, respectively. To demonstrate the capability of the proposed method the sheet resistance of a continuous 2 nm Ni film (>950 Ω/□) is reduced to ~6.5 Ω/□ when a 100 nm thick Cu grid is deposited on it. The transparency is instead maintained at values exceeding 75%. These results, which can be further improved by making thicker grids, already demonstrate the potential in applications, such as photovoltaic cells, optical detectors and displays.
 [doi:10.1063/1.3299259]

Transparent electrodes (TEs) are essential elements in a wide range of optoelectronics devices, such as organic LEDs, photovoltaic cells, and liquid crystal displays. From an application point of view, besides large optical transparency in the wavelength range of interest and adequate electrical conductivity, TEs should possess other key features, such as compatibility with other materials that form the same device (in particular active layers), stability against temperature, mechanical and chemical stress, easy processing, potential for large scale deposition, and low cost.[1] The state-of-the-art solution consists in wide band gap transparent conductive oxides (TCOs), among which indium tin oxide (ITO) is the most popular. Although ITO has excellent transmission and low sheet resistance, it possesses several drawbacks, for example, high cost due to indium scarcity, need of postdeposition treatments, dependence of performance on doping, deposition conditions, and their multicomponent structure which can lead to incompatibilities with some active materials in devices.[2–5] These facts have led to search for alternative materials, such as single walled carbon nanotubes, graphene films, and ultrathin metal films (UTMFs).[3–7] Among them, UTMFs can overcome the high cost of raw materials and be grown using a simple process technique. Contrary to TCOs, they also possess high compatibility with nearly all organic and semiconductor materials and related device fabrication steps.[4,5] However, if one wants to achieve high optical transmission, the thickness of UTMFs should be limited to several nanometers, at the expense of sheet resistance. For example, 40 nm Ni films can achieve sheet resistance values of less than 5 Ω/□ but are opaque. Similarly, 2 nm Ni UTMF shows transparency over 80%, but their sheet resistance increases to more than 950 Ω/□.[4] In this letter we propose a design and report experimental results which confirm that it is possible to reduce the sheet resistance of UTMF based TEs of more than two orders of magnitude without significantly affecting their transparency. The proposed UTMF based TE (G-UTMF) consists of a uniform UTMF with a top metal grid structure in contact with it. The grid structure that we use to demonstrate the concept is formed of microscale periodically perforated dense metal. However, the concept can be applied to either a different conductive material (semiconductor) or a different geometry (random mesh). By changing the linewidth and the thickness of the grid, the optical transparency and the sheet resistance can be tuned accordingly.

A 2 nm Ni UTMF was room-temperature deposited on a double side polished UV fused silica substrate using 100 W dc power (Ajaint Orion 3 sputtering system) in pure Ar atmosphere at 0.27 Pa. Prior to the deposition the substrate was cleaned with oxygen plasma with a pressure of 1.1 Pa and 40 W rf power for 15 min. After the deposition, a negative photoresist was spin-coated on the film. In fact, the thickness of the photoresist determines the maximum thickness of the metal grid to be deposited later in the process. Using the standard UV lithography (Quintal Q4000 mask aligner) for negative photoresist, a pattern of openings for subsequent deposition of thick metal was defined onto the sample. The process flow is depicted in Fig. 1. Subsequently,

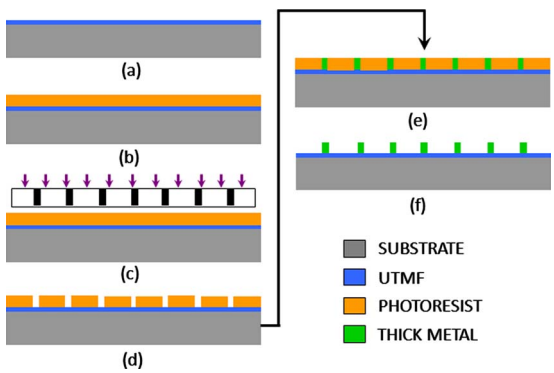

FIG. 1. (Color online) Fabrication steps for a G-UTMF.

[a)]Electronic mail: dhriti.ghosh@icfo.es.
[b)]Electronic mail: tonglai.chen@icfo.es.

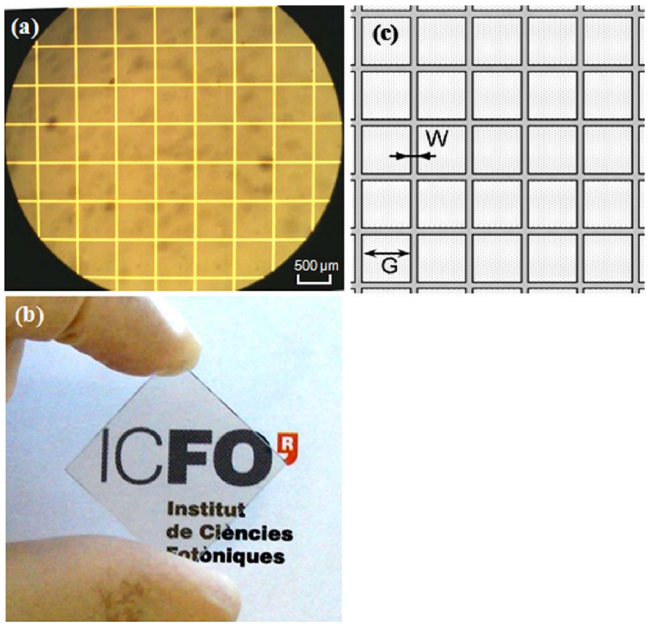

FIG. 2. (Color online) (a) and (b) show the microscopic and macroscopic view, respectively, of a G-UTMF based TE, and (c) a drawing of the grid pattern.

the prepared sample was loaded in the sputtering chamber and a thick metal was deposited using the same aforementioned conditions. After the deposition, the sample was dipped into acetone and placed in an ultrasonic bath till the photoresist was completely lifted off. Figure 2(a) shows a microscope picture of the resulting structure and Fig. 2(b) shows the real appearance of a typical sample with the TE fabricated as described above. The electrical sheet resistance of the obtained G-UTMF and the initial UTMF was measured by van der Pauw method and Four point Probe (Cascade Microtech 44/7S), respectively, as the latter method was found to be not always stable and reproducible for G-UTMF structures. For the transmission spectra, a Perkin Elmer Lambda 950 spectrophotometer was used.

In such a combined structure (G-UTMF), besides contributing to the collection and injection of electrical charges where the grid lines are absent, the underlying UTMF layer can also be used for other functionalities, for example, work function matching with active layers in photovoltaic and LED devices. Since the sheet resistance of the underlying UTMF becomes negligible on a scale larger than the grid period, the overall current distribution is mainly dominated by the metal grid-structure. The sheet resistance of G-UTMF ($R_{S,TOT}$) can be written as (based on Ohm's law) follows:

$$R_{S,TOT} = \xi \frac{\frac{\rho_G}{t_G}\frac{1}{f_F}\left(\frac{\rho_G}{t_G}\frac{W}{G} + \frac{\rho_{UTMF}}{t_{UTMF}}\right)}{\frac{\rho_G}{t_G}\frac{1}{f_F} + \frac{\rho_G}{t_G}\frac{W}{G} + \frac{\rho_{UTMF}}{t_{UTMF}}}, \quad (1)$$

where ρ_G, t_G and ρ_{UTMF}, t_{UTMF} are the resistivity and thickness of the grid and UTMF respectively. ξ is a correction factor, which depends on deposition conditions and can be determined experimentally for a given deposition technique and specific process. "G" is the grid spacing and "W" is the linewidth, [Fig. 2(c)]. f_F is the filling factor, which is defined by $W/(G+W)$. The filling factor thus quantifies the area covered by metal strips compared to UTMF. In fact with good

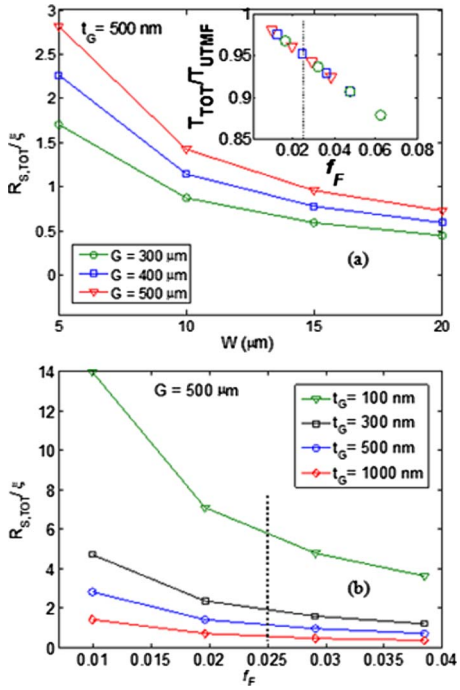

FIG. 3. (Color online) (a) Sheet resistance of G-UTMF as a function of linewidth for different grid spacings (fixed t_G=500 nm). Inset is the variation in transparency against the filling factor. (b) Sheet resistance of G-UTMF as a function of filling factor for different grid Ni thickness (fixed G=500 μm). The dotted lines in the figures correspond to the calculated optimum filling factor.

approximation the sheet resistance of G-UTMF on a scale larger than the period of the grid can be expressed by the following:

$$R_{S,TOT} = \xi \frac{\rho_G}{t_G f_F}. \quad (2)$$

The optical transparency of G-UTMF can be written as follows:

$$T_{TOT} = T_{UTMF} \times (1 - f_F)^2. \quad (3)$$

Note that for simplicity we have assumed that the thickness of metal grid is large enough to make it opaque. From Eq. (3) one can gather that the transparency of G-UTMF is independent of grid metal thickness, only a function of filling factor.

Figure 3(a) shows the calculated dependence of $R_{S,TOT}$ on linewidth for different grid spacing (t_G=500 nm fixed). All these calculations were carried out considering the same material (Ni) for both grid and UTMF. As the grid spacing widens, the sheet resistance slightly goes up due to the decreased filling factor. The influence in f_F on the transparency is shown in the inset of Fig. 3(a), exhibiting a linear behavior over the presented range. Figure 3(b) shows the dependence of $R_{S,TOT}$ on f_F for different grid metal thickness (G =500 μm fixed). With the increase in grid metal thickness, $R_{S,TOT}$ decreases significantly as the conductivity behavior relies on the thick metal grid-structure. From these data it is evident that a trade-off exists between T_{TOT} and $R_{S,TOT}$, which corresponds to an optimum f_F. To define the trade-off we introduce the figure of merit, Φ_{TE}, defined by Haacke[8]

TABLE I. Comparison of experimental results with calculated theoretical values for different G/W ratios. Note that both UTMF and grid are made of Ni.

G/W	25	33	50	100
Experimental data (R_S, T_{TOT})	(28.37, 76.5)	(51.4, 76.67)	(99.3, 76.83)	(197.16, 80.37)
Calculated data (R_S, T_{TOT})	(52.02, 74.25)	(67.7, 75.87)	(101.3, 77.2)	(197.76, 78.73)

$$\Phi_{TE} = \frac{T_{TOT}^{10}}{R_{S,TOT}}. \quad (4)$$

Using Eqs. (2) and (3), Eq. (4) can be rewritten as

$$\Phi_{TE} = \frac{t_G \times T_{UTMF}^{10} \times f_F \times (1-f_F)^{20}}{\xi \times \rho_G} = B \times f_F \times (1-f_F)^{20}, \quad (5)$$

where B can be viewed as a constant for a given grid thickness, which equals to $[t_G \times T_{UTMF}^{10}/(\xi \times \rho_G)]$. Considering the small value of $f_F(\ll 1)$, Eq. (5) can be simplified by using Newton's binomial theorem as follows:

$$\Phi_{TE} \approx B(f_F - 20f_F^2). \quad (6)$$

For this quadratic equation, the value of filling factor for which the Φ_{TE} is maximized can be calculated as follows:

$$\frac{\partial \Phi_{TE}}{\partial f_F} = B(1-40f_F) = 0,$$

$$f_F = \frac{1}{40} = 0.025. \quad (7)$$

From the definition of f_F, for the highest Φ_{TE}, the ratio of spacing to linewidth should equal 39. Moreover, one can further tune sheet resistance by proper choice of grid thickness, t_G and different metal materials.

To experimentally assess the proposed design, we fabricated four samples of different linewidth (5, 10, 15, and 20 μm), with fixed $G=500$ μm and $t_G=50$ nm. Both UTMF and grid are made of Ni. According to our deposition conditions, the value of ξ is determined as 7.2. Table I compares the calculated and experimental data, which show good agreement with each other for large G/W values. For small G/W values the approximation condition in Eq. (2) starts not being valid any longer. However, the above-mentioned equations help to design and predict the performance of G-UTMF based TEs. Note that the grid thickness employed in Table I is fixed at 50 nm. One can multiply the grid thickness and choose other metals (such as copper, silver, or gold) to scale down the sheet resistance to below 10 $\Omega/\square$ without compromising the transparency. To demonstrate this possibility we have fabricated a G-UTMF sample made of 100 nm Cu grid +2 nm Ni UTMF and achieved a sheet resistance of about 6.5 $\Omega/\square$ and optical transparency exceeding 75%, the latter being similar to the all Ni G-UTMF (same pattern). Figure 4 shows the wavelength dependence of the transparency of the Ni UTMF, Ni/Cu G-UTMF and, for comparison, of a standard ITO film. One can readily appreciate that the transparency of all the films is similar in the visible region while it is much higher for the metal based TEs in the UV and infrared, the latter aspect being crucial in several applications (e.g., UV and infrared detectors and photovoltaic cells for space).

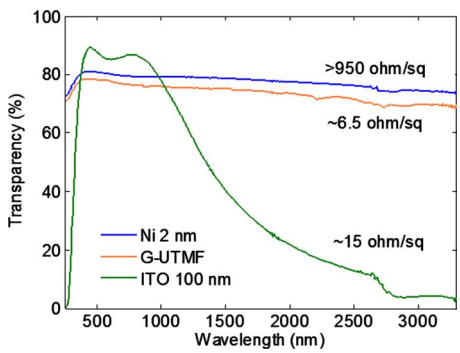

FIG. 4. (Color online) Comparison of optical transparency for UTMF (2 nm Ni), G-UTMF (2 nm Ni+100 nm Cu grid), and 100 nm ITO. The corresponding sheet resistances are also indicated in the figure. The substrate contribution is taken into account in optical transmittance measurements as $T_F = T_{TOT}/T_S$, where T_F is the deposited film transparency, T_{TOT} is the total optical transmittance (film and substrate), and T_S is the substrate optical transmittance.

In summary, by incorporating a thick metal grid on the top of UTMF, we have demonstrated an effective approach to reduce significantly (more than two orders of magnitude) the electrical sheet resistance of metal based TEs, with negligible loss in optical transparency. The theoretical calculation showed that the value of filling factor and the ratio of grid spacing to linewidth should be around 0.025 and 39, respectively, to achieve the highest Φ_{TE}. Further tailoring in optical and electrical properties of the proposed G-UTMF based TEs can be achieved by using different materials and grid geometry. Note also that the grid or mesh structure could be deposited using inexpensive techniques, such as screen printing and shadow masking during deposition. We believe that, because of their process simplicity and low cost, the proposed structures will have an impact in a wide range of applications, including photovoltaic cells, optical displays, detectors and electrochromic devices.

This work was partially supported by the Generalitat de Catalunya ACC1Ó program and the Spanish National Program Plan Nacional Grant No. TEC 2007-60185.

[1] C. G. Granqvist, Sol. Energy Mater. Sol. Cells **91**, 1529 (2007).
[2] B. O'Connor, C. Haughn, K. H. An, K. P. Pipe, and M. Shtein, Appl. Phys. Lett. **93**, 223304 (2008).
[3] Y. Wang, X. Chen, Y. Zhong, F. Zhu, and K. P. Loh, Appl. Phys. Lett. **95**, 063302 (2009).
[4] D. S. Ghosh, L. Martinez, S. Giurgola, P. Vergani, and V. Pruneri, Opt. Lett. **34**, 325 (2009).
[5] D. Krautz, S. Cheylan, D. S. Ghosh, and V. Pruneri, Nanotechnology **20**, 275204 (2009).
[6] Z. Wu, Z. Chen, X. Du, J. M. Logan, J. Sippel, M. Nikolou, K. Kamaras, J. R. Reynolds, D. B. Tanner, A. F. Hebard, and A. G. Rinzler, Science **305**, 1273 (2004).
[7] X. Wang, L. Zhi, and K. Mullen, Nano Lett. **8**, 323 (2008).
[8] G. Haacke, J. Appl. Phys. **47**, 4086 (1976).